Electronic Supplementary Information (ESI†)

Generation of maghemite nanocrystals from iron-sulfur centres

Samya Banerjee,[a] Andreas Omlor,[b] Juliusz A. Wolny,[b] Yisong Han,[c] Frederik Lermyte,[a,d] Amy E. Godfrey,[a] Peter B. O'Connor,[a] Volker Schünemann,[b] Mohsen Danaie,*[e] and Peter J. Sadler*[a]

[a] *Department of Chemistry, University of Warwick, Gibbet Hill Road, Coventry CV4 7AL, United Kingdom, P.J.Sadler@warwick.ac.uk*

[b] *Department of Physics, Technische Universität Kaiserslautern , Erwin-Schrödinger-Straße 46, 67663 Kaiserslautern, Germany*

[c] *Department of Physics, University of Warwick, Gibbet Hill Road, Coventry CV4 7Al, United Kingdom*

[d] *School of Engineering, University of Warwick, Gibbet Hill Road, Coventry CV4 7Al, United Kingdom*

[e] *Diamond Light Source Ltd, electron Physical Science Imaging Centre (ePSIC), Harwell Science & Innovation Campus, Didcot, Oxfordshire OX11 0DE, U.K, mohsen.danaie@diamond.ac.uk*

Contents

1. Materials and Methods

Anhydrous iron(III) chloride ($FeCl_3$), toluene-3,4-dithiol, Pluronic® P123, anhydrous tetrahydrofuran, methanol were all purchased from Sigma-Aldrich and used as received. Triethylamine was purchased from Fisher Scientific, and dialysis membranes from. Spectrum Laboratories, Inc., Spectra/Por®6; MWCO 1 kDa (flat width 45 mm, diameter 29 mm, vol/length 6.4 mL/cm). Pure water (18.2 MΩ) was from a Purelab UHQ USF Elga system. Lacey carbon copper grids with 200 mesh were purchased from Agar Scientific.

ESI-MS analysis was carried out on an Agilent Technologies 1100 Quadrupole MS instrument. High resolution mass spectra were obtained from a Bruker MaXis plus Q-TOF mass spectrometer equipped with electrospray ionisation source. The instruments were used in negative ion mode.

1. Synthesis of [Fe(4-methyl-1,2-benzenedithiolate)$_2$][NHEt$_3$] (1)

Toluene-3,4-dithiol (0.4 mmol, 0.063 g) was treated with 2 mol equiv of Et_3N (0.8 mmol, 0.08 g) in 5 ml of MeOH to deprotonate the thiol groups. The resulting solution was subsequently added dropwise to a stirred solution of anhydrous iron(III) chloride (0.2 mmol, 0.033 g) in 10 mL of methanol, accompanied by a colour change from yellow to black followed by formation of a black precipitate. The precipitate was collected by filtration, washed with MeOH, and dried under vacuum. Yield: 71.9 %. Anal: Calc for $C_{20}H_{28}NS_4Fe$; C: 51.49, H: 6.05, N: 3.00; S: 27.49 Found C: 51.21, H: 6.13, N: 3.21, S: 27.30. ESI-MS: Calc for $[C_{14}H_{12}S_4Fe]^-$= 363.9; found 363.9; confirmed by HRMS: 363.9181.

DFT Calculations

Complex **1** appears to be a structural analogue of bis(o-xylyldithiolato)ferrate(III) monoanion.[1] Yet the isomer shift for **1** (0.48 mm s^{-1}**)** is significantly higher than that of 0.13 mm s^{-1} (at 77K) observed for the latter complex, suggesting that the molecular structure of complex **1** does not have a high-spin tetrahedral Fe(III)S_4 coordination core. Therefore we performed DFT modelling for three models of the title cation: high-spin tetrahedral, high-spin square-planar and low-spin square-planar. B3LYP/CEP-31g optimisations and frequency calculations were performed with Gaussian16[2], the Mössbauer parameters were calculated with ORCA[3] (B3LYP/CP(PPP)).

The calculated electronic energies point towards stabilization of the tetrahedral form, with low-spin and high-spin square-planar configurations lying 51 and 38 kJ mol^{-1} above it. The results are given in Table S3, with the calculated and experimental far infrared spectra in Fig. S2.

When complex **1** was optimized as a whole (with counter cation), a strained high-spin tetrahedral structure was generated in which the proton of $NHEt_3^+$ is hydrogen-bonded to one of the Fe(III) coordinated sulfurs with an H-bond distance of 2.09 Å (Fig. S3). The three Fe-S bond distances are 2.32-2.34 Å, higher than reported for the bis(o-xylyldithiolato)ferrate(III) monoanion (2.25-2.28 Å)[1]. The Fe-S (H-bonded to $HNEt_3^+$) is 2.39 Å, significantly longer than

other three Fe-S bonds in the structure. The two S-Fe-S bond angles are ca. 94° whereas the other two S-Fe-S bond angles are ca. 109°. In bis(o-xylyldithiolato)ferrate(III), the S-Fe-S bond angles were ca. 106-113°.[1] The DFT data indicate that complex **1** might be more strained than that of bis(o-xylyldithiolato)ferrate(III).

Scanning Transmission Electron Microscopy

High-resolution scanning electron microscopy was performed on a probe aberration-corrected JEOL ARM 200F, operated at 80 keV accelerating voltage. For imaging, we used 40 μm probe-forming aperture resulting in 30.5 mrad probe convergence half-angle and high-angle annular dark-field detector at 4 cm camera length, collecting scattered electrons between 120 and 410 mrad. This microscope is equipped with two JEOL x-ray energy-dispersive spectroscopy (EDX) detectors with ~1.5 strad combined collection angle and a Quantum GIF for electron energy loss spectroscopy (EELS). EDX and EELS spectrum images were acquired at similar optical condition, with the probe current of 88 pA (spot size 5C). Initially the scanning electron beam caused significant carbon contamination build-up on the sample. This was mitigated by illuminating a large area of the sample with the 150 μm probe-forming aperture and highly defocused sample with a stationary beam of around 9.6 nA for 5 min. This illumination period was also used to trigger electron beam-induced structural changes in the micelles.

Transmission Electron Microscopy

TEM experiments were performed on a JEOL JEM-2100plus microscope operated at 80 keV.

Table S1: Calculated versus observed *m/z* values for the major isotope peaks of $[C_{14}H_{12}S_4Fe]^-$.

m/z (calc)	m/z (observed)	Δ(Da)	ppm error
361.9223	361.9224	0.0001	0.2
362.9257	362.9258	0.0001	0.2
363.9177	363.9174	-0.0003	-0.9
364.9210	364.9210	-0.0001	-0.2
365.9135	365.9133	-0.0001	-0.4
366.9168	366.9169	0.0001	0.1
367.9092	367.9094	0.0002	0.5

Table S2: Calculated versus observed *m/z* values for the major isotope peaks of $[C_{19}H_{38}ClO_4]^-$ (the most plausible source of the contaminant signals between 365 and 368 Da, based on accurate mass measurement shown here and the matching isotope pattern shown in Fig. S1).

m/z (calc)	m/z (obs)	Δ (Da)	ppm error
365.24641	365.24610	-0.00031	-0.8
366.24977	366.24965	-0.00012	-0.3
367.24346	367.24328	-0.00018	-0.5
368.24682	368.24685	0.00003	0.1

Table S3: Mössbauer parameters for **1** obtained from data collected at 77 K and results of DFT calculations.

Model compound/ geometry	Experimental			Theoretical	
	δ (mm/s)	ΔE_Q (mm/s)	Γ (mm/s)	δ (mm/s)	ΔE_Q (mm/s)
1	0.47	0.76	0.48		
tetrahedral				0.33	1.3
tetrahedral opt. with cation				0.31	1.4
square-planar high-spin				0.49	2.77
square-planar low-spin				0.48	0.47

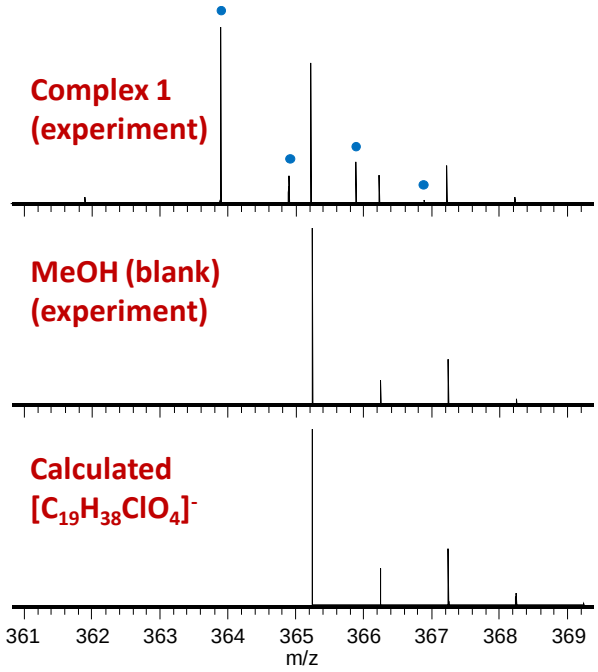

Fig. S1: Identification of contaminant peaks in FTMS: **top,** complex **1** (labelled with blue dots, as in the main text), **middle**, methanol alone, and **bottom**, the theoretical isotope distribution for $[C_{19}H_{38}ClO_4]^-$.

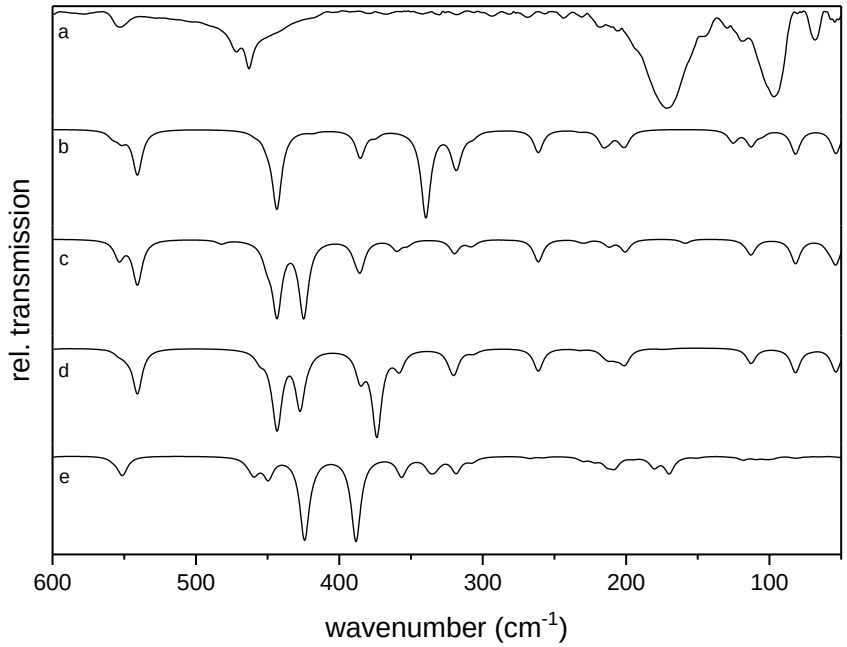

Fig. S2: a) Experimental IR spectrum of **1**, b) DFT-calculated IR spectrum assuming a square-planar high-spin conformation, c) DFT calculated IR spectrum assuming a square-planar low-spin geometry, d) DFT calculated IR spectrum assuming a tetrahedral high-spin geometry and e) DFT calculated IR spectrum starting from a tetrahedral high-spin complex with NEt_3H^+ cation. In cases b)- d) the simulated spectrum is the sum of DFT calculated vibrations for the isolated complexes and the NEt_3H^+ cation.

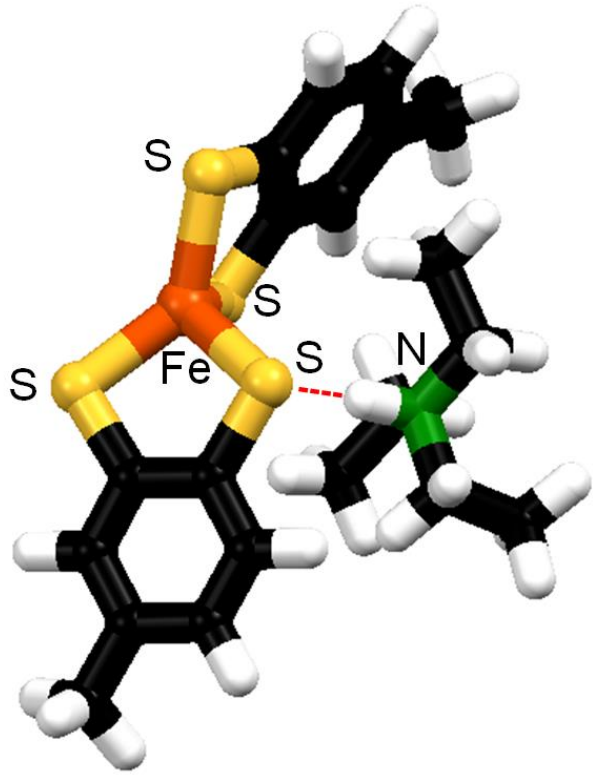

Fig. S3: Energy optimized structure of the complex **1.** The S---$HNEt_3^+$ H-bonding interaction is indicated by a red dotted line.

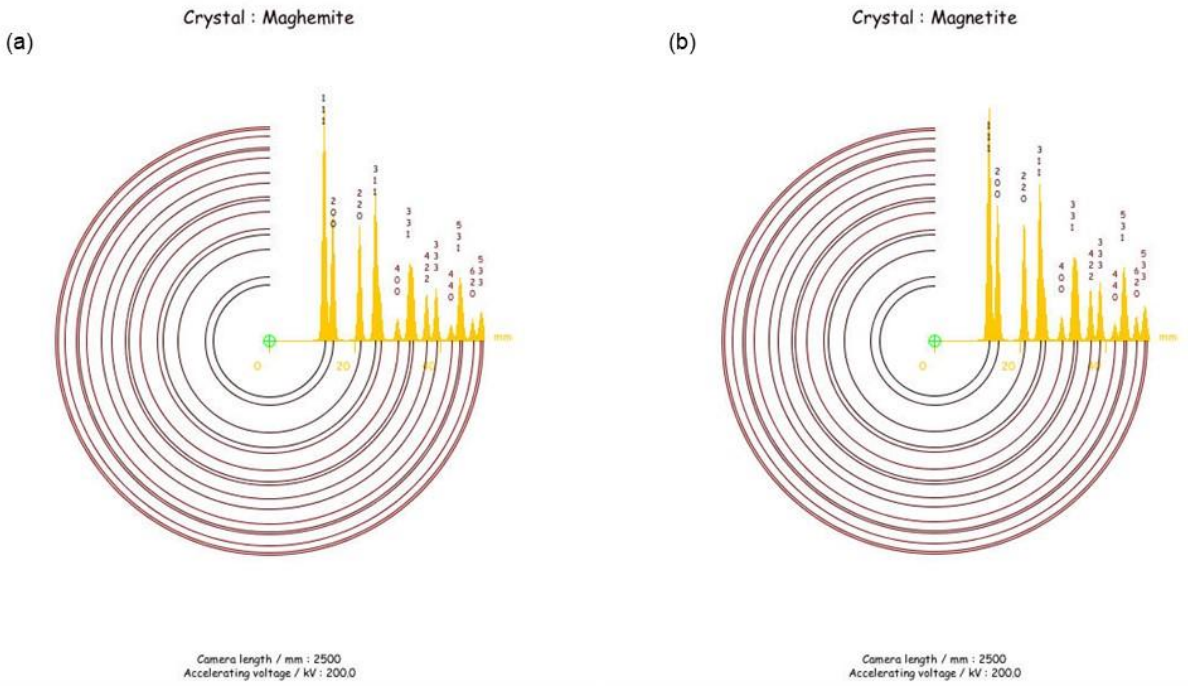

Magnetite

h	k	l	Dist. nm-1	Dist. nm	Rel. Int.
1	1	1	2.063	0.48473	1000
2	0	0	2.38214	0.41979	564
2	2	0	3.36886	0.29684	501
3	1	1	3.95034	0.25314	653
2	2	2	4.12599	0.24237	193
4	0	0	4.76429	0.20989	96
3	3	1	5.19176	0.19261	301
4	2	0	5.32663	0.18774	279
4	2	2	5.83504	0.17138	214

Maghemite

h	k	l	Dist. nm-1	Dist. nm	Rel. Int.
1	1	1	2.07929	0.48093	1000
2	0	0	2.40096	0.4165	561
2	2	0	3.39547	0.29451	489
3	1	1	3.98154	0.25116	631
2	2	2	4.15859	0.24047	186
4	0	0	4.80192	0.20825	91
3	3	1	5.23277	0.1911	282
4	2	0	5.36871	0.18626	261
4	2	2	5.88113	0.17004	198

Fig. S4: Simulated electron diffraction patterns for polycrystalline (a) maghemite and (b) magnetite, with corresponding reflection intensities inset in each case. The Table gives the d-spacing values in each case. Simulation was carried out using JEMS[4] and the cif files from the crystallography database.

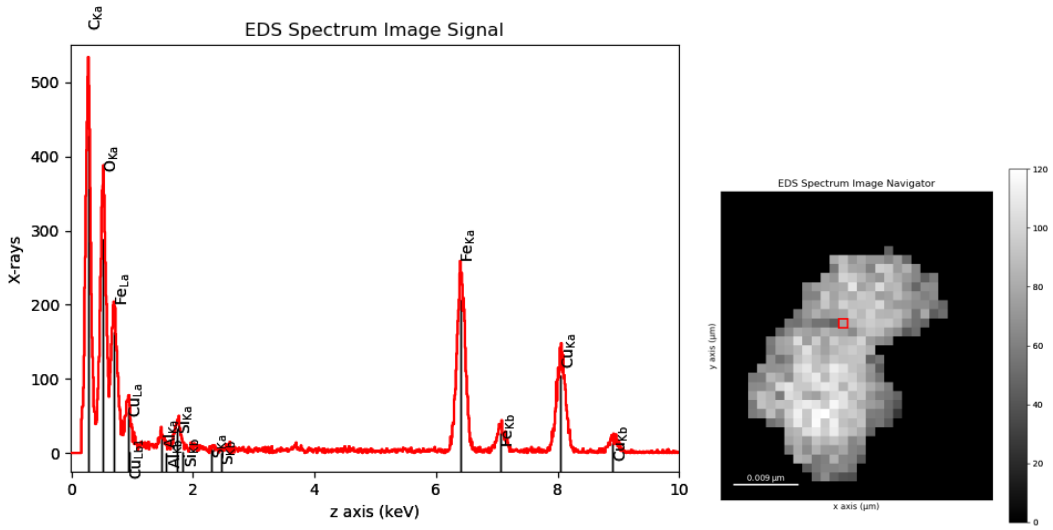

Fig. S5: EDX sum spectrum of the masked Fe-rich particle (shown on the right hand side). Quantification using HypeSpy package[5] resulted in the following atomic ratios: Fe:O:C = 1:3.6:12.3. The high oxygen content can be attributed to some of the oxygen being bonded to carbon rather than the Fe ions.

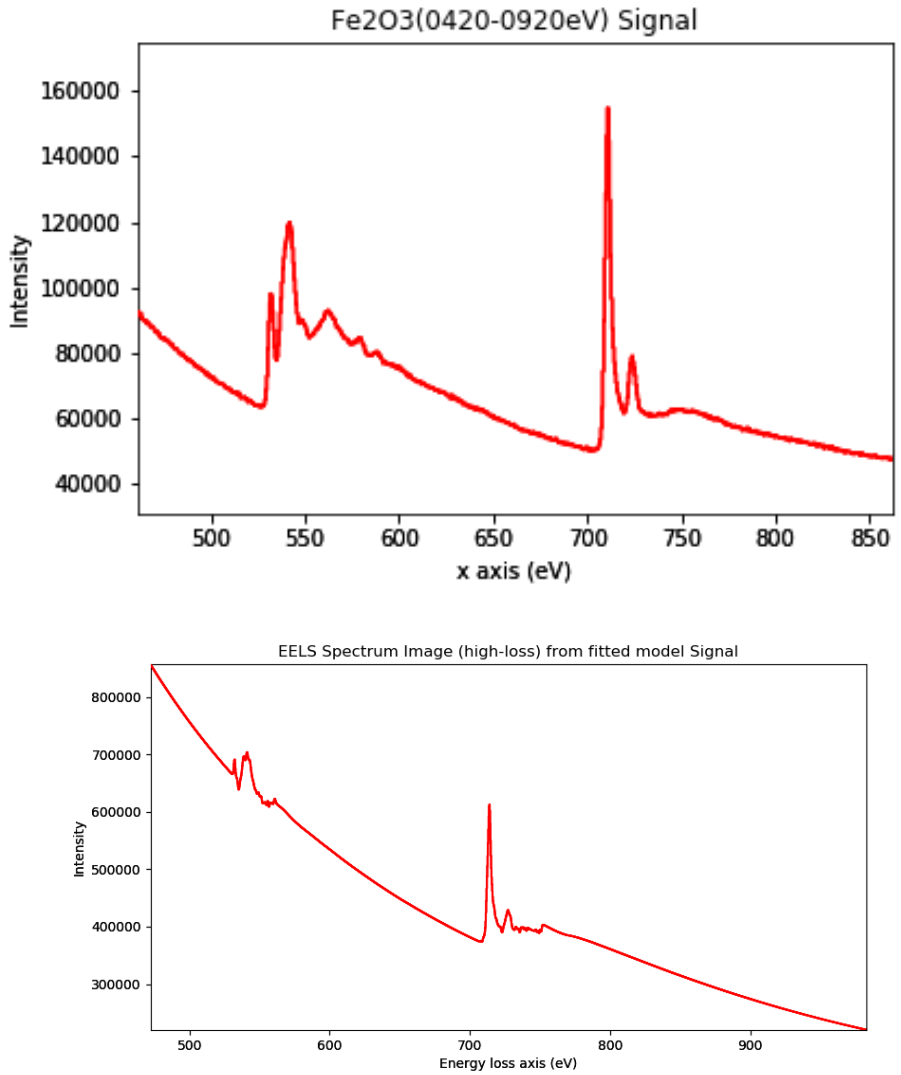

Fig. S5: Experimental EELS spectrum of Fe_2O_3 from reference material[6] (top) and EELS model fitted to the experimental data (bottom) using HyperSpy (using the fine structure module)[5].

Reference:

1. R. W. Lane, J. A. Ibers, R. B. Frankel and R. H. Holm, *Proc. Nat. Acad. Sci. USA*, 1975, **72**, 2868.
2. Gaussian 16, Revision A.03, M. J. Frisch, G. W. Trucks, H. B. Schlegel, G. E. Scuseria, M. A. Robb, J. R. Cheeseman, G. Scalmani, V. Barone, G. A. Petersson, H. Nakatsuji, X. Li, M. Caricato, A. V. Marenich, J. Bloino, B. G. Janesko, R. Gomperts, B. Mennucci, H. P. Hratchian, J. V. Ortiz, A. F. Izmaylov, J. L. Sonnenberg, D. Williams-Young, F. Ding, F. Lipparini, F. Egidi, J. Goings, B. Peng, A. Petrone, T. Henderson, D. Ranasinghe, V. G. Zakrzewski, J. Gao, N. Rega, G. Zheng, W. Liang, M. Hada, M. Ehara, K. Toyota, R. Fukuda, J. Hasegawa, M. Ishida, T. Nakajima, Y. Honda, O. Kitao,

H. Nakai, T. Vreven, K. Throssell, J. A. Montgomery, Jr., J. E. Peralta, F. Ogliaro, M. J. Bearpark, J. J. Heyd, E. N. Brothers, K. N. Kudin,. N. Staroverov, T. A. Keith, R. Kobayashi, J. Normand, K. Raghavachari, A. P. Rendell, J. C. Burant, S. S. Iyengar, . Tomasi, M. Cossi, J. M. Millam, M. Klene, C. Adamo, R. Cammi, J. W. Ochterski, R. L. Martin, K. Morokuma, O. Farkas, J. B. Foresman, and D. J. Fox, Gaussian, Inc., Wallingford CT, 2016.

3. F. Neese, The ORCA program system, Wiley Interdiscip. Rev.: Comput. Mol. Sci., 2012, **2**, 73.
4. http://www.jems-saas.ch/
5. F. de la Peña *et al*, (2018, October 23). hyperspy/hyperspy v1.4.1 (Version v1.4.1). Zenodo. http://doi.org/10.5281/zenodo.1469364.
6. C. C. Ahn, O. L. Krivanek, M. M. Disko, EELS atlas: a reference collection of electron energy loss spectra covering all stable elements. HREM Facility, Center for Solid State Science, Arizona State University; 1983.